Passive control of the stability of aircraft wing and blade turbine

M. Hamadiche
Laboratoire de mécanique des fluides et d'acoustique,
Ecully, 36134, France
email: mahmoud.hammadich@gmail.com

Abstract

The stability of blades and wings is considered in this work, the natural modes of the thin blades and wings in incidence under the action of aerodynamic forces are computed. The wing in this study has two degrees of freedom corresponding to the bending and torsion. The variation of the unstably modes versus the far flow field velocity is predicted, in particular, the effects of the variation of the chord on the stability is examined . Wing stabilization by piezoelectric material are considered.

Aeroelasticity, blade, wing, piezoelectric

Introduction

The airfoils and plades are involved in many applications nowadays, wind turbine, commercial air planes, turbines, compressor, fans, rotors and propellers are not the unique examples. The flow around an airfoil and blade depend on the geometrical configuration of the airfoil and the nature of the flow in far field. For a stable wing of small angle of attack the flow is attached to the wing and the oscillation of the lift and consequently the vibration of the wing are mainly imposed by turbulence density of far field free stream. When the angle of attack exceeds its critical values the flow is no longer attached to the wing and the flow separation occurs a phenomenon associated with a dramatic fall on the lift. If the angle of attack is increased farther the wing behave like a bluff body generating a structure similar to the classic kármán vortex street. The frequency of the shedding vortex increases with the increase of the free stream velocity and decreases with the increase of the angle of attack and the amplitude of the oscillation are lock-in with the frequency of shedding vortex [1,2].

Controlled strain-induced blade twisting can be attained using piezoelectric Active Fiber Composite technology, aimed at provide a mechanism for reduced rotorcraft vibrations and increased rotor performance [3]. An optimization technique is proposed in order to select the optimal design variables like the thickness of each composite layer, center of gravity of the cross section , shear center, mass per unity length, chord and ballast mass allowing optimal active twist rotors [4]

An passive control strategy for blades disk interaction in compressor and turbine using piezoelectric shunt damping technique is feasible, the strategy is to place the piezoelectric transducers outside the main stream in turbo machinery so that the flow is not perturbed [5], An optimization technique is employed in order to place the piezoelectric shunt at optimal locations [5]. In the case of a high aspect ratio low-pressure turbine blade the unstable bladed disk reaches a state in which only a single travelling wave exists [6]. In this work we shall show how to control the stability of the air foil passively. In particular we shall examine the effects of the chord shrinking and the effects of added piezoelectric material.

Formulation of the problem

Vibration control based on the passive piezoelectric shunt damping technique has been documented in the literature [5]. In this paragraph, we shall present an example to show how piezoelectric shunt can be used to delay the threshold instability of blade of airfoil. Let some piezoelectric material be inserted in a wing or in a blade, so that the wing motion is coupled to two electrical circuits powered by the piezoelectric material, the equation of motion become,

$$\frac{\partial^2}{\partial x^2}(EI\frac{\partial^2 w}{\partial x^2}) + \varrho S(\frac{\partial^2 w}{\partial t^2} - z_\alpha \frac{\partial^2 \theta}{\partial t^2}) - K_1 q_1 = f \quad (1)$$

$$\frac{\partial}{\partial x}(GJ\frac{\partial \theta}{\partial x}) - I_\alpha \frac{\partial^2 \theta}{\partial t^2} + \varrho S z_\alpha \frac{\partial^2 w}{\partial t^2} = -m_e - K_2 q_2 \quad (2)$$

$$L_1 \frac{\partial^2 q_1}{\partial t^2} C_p q_1 + R_1 \frac{\partial q_1}{\partial t} - K_1 \frac{\partial w}{\partial t} = 0 \quad (3)$$

$$L_1 \frac{\partial^2 q_2}{\partial t^2} C_p q_2 + R_2 \frac{\partial q_2}{\partial t} - K_2 \frac{\partial \theta}{\partial t} = 0 \quad (4)$$

$$f = \rho c \pi U_\infty^2 [\theta - (\frac{L}{U_\infty} - \frac{3c}{4U_\infty})\frac{\partial \theta}{\partial t} - \frac{1}{U_\infty}\frac{\partial w}{\partial t}] \quad (5)$$

$$m_e = \rho \pi U_\infty^2 c^2 [(\frac{1}{4} - \frac{L}{C})(\theta + \frac{1}{U_\infty}(C - L)\frac{\partial \theta}{\partial t} - \frac{1}{U_\infty}\frac{\partial w}{\partial t}) + \frac{L}{4U_\infty}\frac{\partial \theta}{\partial t}] \quad (6)$$

where the two constant K_1 and K_2 are reflecting the electro-mechanical coupling effects, L_1 and L_2, R_1 and R_2, are the inductance of and the resistances of the two electrical circuits respectively, U_{infty} is the far field flow velocity, w is the displacement of the elastic axis and θ is

the angle of rotation around the elastic axis. L is the position of the elastic axis, E is the Young modulus and G is the shear modulus. Z_α is the position of the mass center axis, ϱ and ρ are the mass density of the solid and fluid. f and m_e are the aerodynamic force and moment at the elastic axis by unity length. The solution of the system of partial differential equations is sought in the form of a normal mode, i.e.

$$[w, \theta, q_1, q_2] = [w_\omega, \theta_\omega, q_1^\omega, q_2^\omega]e^{i\omega t} \quad (7)$$

The equation of motion become

$$\frac{\partial^2}{\partial x^2}(EI\frac{\partial^2 w_\omega}{\partial x^2}) - \omega^2 \varrho S(w_\omega - z_\alpha \theta_\omega) - K_1 q_1 = f_\omega \quad (8)$$

$$\frac{\partial}{\partial x}(GJ\frac{\partial \theta_\omega}{\partial x}) + \omega^2 I_\alpha \theta - \omega^2 \varrho S z_\alpha w_\omega = -m_e^\omega - K_2 q_2^\omega \quad (9)$$

$$-\omega^2 L_1 q_1^\omega + C_p q_1 + i\omega R_1 q_1^\omega - i\omega K_1 w_\omega = 0 \quad (10)$$

$$-\omega^2 L_1 q_2^\omega + C_p q_2^\omega + i\omega R_2 q_2^\omega - i\omega K_2 \theta_\omega = 0 \quad (11)$$

$$f^\omega = \rho c \pi U_\infty^2 [\theta - i\omega(\frac{L}{U_\infty} - \frac{3c}{4U_\infty})\theta_\omega - \frac{i\omega}{U_\infty} w_\omega] \quad (12)$$

$$m_e^\omega = \rho \pi U_\infty^2 c^2 [(\frac{1}{4} - \frac{L}{C})(\theta_\omega + \frac{i\omega}{U_\infty}(C - L)\theta_\omega - \frac{i\omega}{U_\infty} w_\omega) + \frac{i\omega L}{4U_\infty}\theta_\omega] \quad (13)$$

The boundary condition associated to the above system are

$$\theta_\omega = w_\omega = \frac{\partial w_\omega}{\partial x} = 0 \quad ; \quad \text{at x=0} \quad (14)$$

$$\frac{\partial \theta_\omega}{\partial x} = \frac{\partial^2 w_\omega}{\partial x^2} = \frac{\partial^2 w_\omega}{\partial x^3} = 0 \quad ; \quad \text{at x=l} \quad (15)$$

l is the length of the wing. The above system is transformed to a first order differential system composed of six first order differential equations. Then, forth order Range-Kutta method is used to obtain three linearly independent solutions obeying to the boundary condition at $x = 0$. The boundary condition at $x = l$ are used to find ω, i.e. the eigenvalues of the system.The shouting method is used to compute the eigenvalues of the above system, namely ω satisfying the boundary condition at $x = l$. Some results are are shown in figure 1 and 2

Results and conclusion

Numerical analysis shows that there are two unstable modes of equal amplification rate (imaginary part of ω) and opposite frequency (real part of ω). The system becomes unstable when the the imaginary part of ω is negative. Figure 1 shows these modes for three values of the parameter of control versus far field flow velocity (the two modes are plotted three times). In this figure the imaginary part of the two unstable modes are superimposed and can be seen as one curve. Note that for large flow velocity the two modes coalesce to form one mode, i.e. a double root of the dispersion equation. Figure 1 shows the effect of narrowing the chord of the wing noted C on the unstable modes where the two unstable modes are plotted versus the far field flow velocity for some values of wing shape. The narrowing the wing is given by the equation

$$C = C_0 + (C_l - C0)\frac{x}{l} \quad (16)$$

Figure 1 shows the two unstable modes for $C_l = C_0 = 2m$, $C_l = 0.94C_0$ and $C_l = 0.89C_0$. Note that the critical velocity increases with the decrease of C_l, we conclude that shrinking the chord stabilizes the system. Note that the instability occurs after the stable flatter modes coalesce to form one divergent unstable mode. Figure 2 compare the the two unstable modes obtained without adding piezoelectric material (the most unstable mode) and after adding piezoelectric material (the most stable one). It is concluded that adding piezoelectric material to wing delay the critical velocity as it shown in Figure 2.

https://cmm2017.sciencesconf.org/

Reference

[1] Tang, D. M., and Dowell, E. H.,2014, "Experimental aerodynamic response for and oscillating airfoil in buffeting flow," AIAA journal, Vol. 52, No. 6 June, pp. 2427-2439.

[2] Tang, D. M., and Dowell, E. H.,2007, "Aerodynamic loading for an airfoil with an oscillating Gurney flap," AIAA journal, Vol. 44, No. 4, pp. 1245-1257.

[3] Wilbur, M. L., Mirick, P. H., Yeager, W. T., Langston, C. W., Cesnik, C.E. S. and Shin, S., 2002, "Vibratory Loads Reduction Testing of the NASA/Army/MIT Active Twist Rotor," Journal of the American Helicopter Society, Vol. 47, No. 2, pp. 123-133

[4] Kumar, D. and Cesnik C. E. S., 2015, "New optimization strategy for design of active twist rotor," AIAA journal, Vol. 53, No. 2, pp. 436-448.

[5] Zou, B. Thouverez, F. and Lenoir, D., 2014, "Vibration reductionb of mistuned bladed disk by passive piezo-

electric shunt damping technique," AIAA journal, Vol. 52, No. 6, pp. 1194-1206.
[6] Corral, R. and Gallardo, J. M., 2014,' "Nonlinear dynamics of blade disk with multiple unstable modes," AIAA journal, Vol. 52, No. 6, pp. 1124-1132.

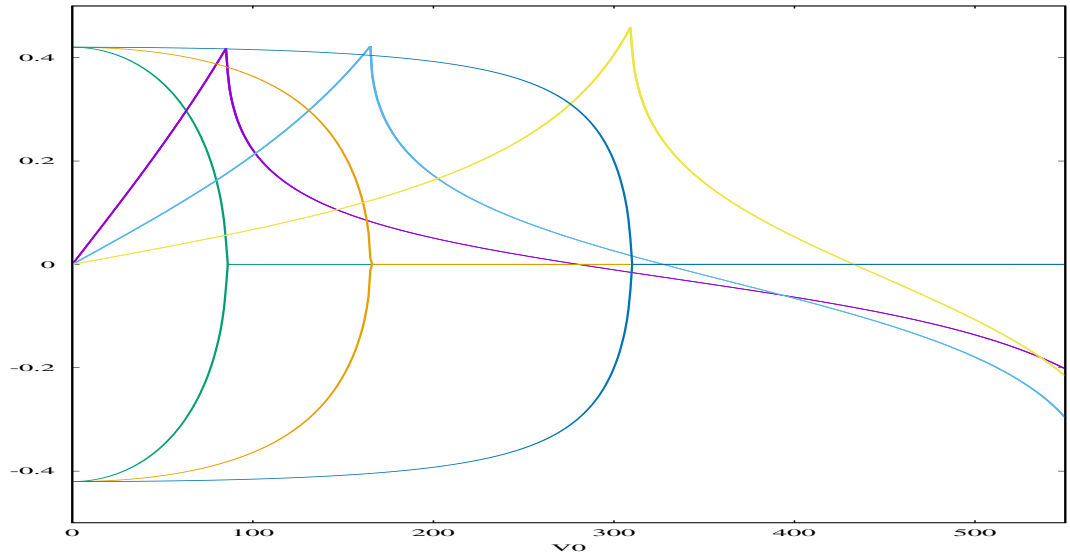

Figure 1: Stabilization due to the shrinking of the chord. Real and imaginary part of ω versus the far field flow velocity. The three symmetric curves are the real part of ω (the frequency) and the edged curve are the imaginary part of ω (Amplification rate). The wing becomes unstable when the imaginary part becomes negative.

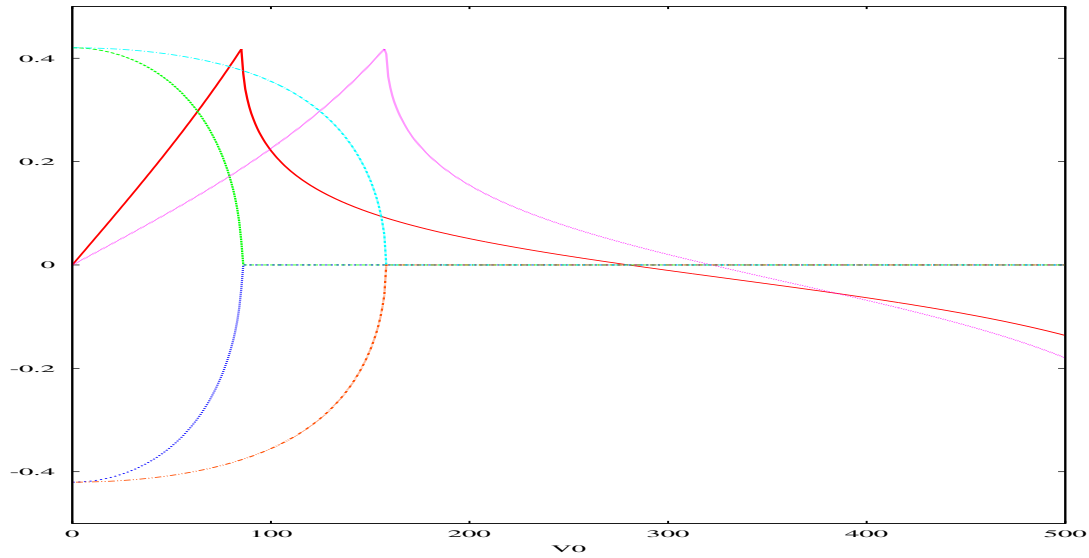

Figure 2: Stabilization due to the added piezoelectric material. Real and imaginary part of ω versus the far field flow velocity. The three symmetric curves are the real part of ω (the frequency) and the edged curve are the imaginary part of ω Amplification rate). The wing becomes unstable when the imaginary part becomes negative.